ICES Journal of Marine Science, 63: 1438–1452 (2006)
doi:10.1016/j.icesjms.2006.03.027

Applying an alternative method of echo-integration

Magnar Aksland

Aksland, M. 2006. Applying an alternative method of echo-integration. – ICES Journal of Marine Science, 63: 1438–1452.

Estimators of mean Echo Value Constant (the ratio between echo abundance and the number of fish) in an alternative echo-integrating method were tried with the SIMRAD EK 60 split-beam echosounder. The mean fish-density estimates of NE Arctic cod were compared with corresponding estimates by the classical echo-integration method; the two methods gave similar results. The alternative method uses integrated single-fish echoes, and a new algorithm to extract and integrate single-target echoes is introduced and used. This algorithm uses echo shape and angle stability, not echo amplitude, to test for the presence of single-target echoes. Apparent single-target echoes with a dynamic range of 60 dB in integrated echo intensity were extracted.

Keywords: echo-integration, estimation of fish abundance, fisheries acoustics, *in situ* method, NE Arctic cod.

Received 15 February 2005; accepted 6 March 2006.

M. Aksland: Department of Biology, University of Bergen, PO Box 7800, N 5020 Bergen, Norway; tel: +47 55584479; fax: +47 55584450; e-mail: magnar.aksland@bio.uib.no.

Introduction

Aksland (2005) described an alternative theory of acoustic-abundance estimation. The basic concepts of this method were presented 30 years ago (Aksland, 1976). Although the method has been applied using target strengths of anaesthetized fish (Aksland, 1983), estimators based on single-target echoes and corresponding directions between transducer and the targets (their detection angles relative to the vertical) have not been applied. With the present widespread use of split-beam echosounders which detect the off-acoustic-axis angles to the targets of resolved echoes, the method of abundance estimation given in Aksland (2005) can be used. The method is based on two basic concepts referred to as echo abundance and the Echo Value Constant, respectively. Both concepts are defined as the area integral of the integrated signal with 20 log R TVG from one ping as a function of the horizontal transducer position. Unlike the concepts of the classical echo-integration method, these concepts are explicitly expressed in terms of the space where the transducer is free to be moved; a horizontal area in the sea under which fish populations are distributed. The simple logic of the method is that the ratio between the echo abundance of a population and its mean Echo Value Constant is equal to the number of individuals in the population, as proved in Aksland (1986).

Two different types of estimator for the mean Echo Value Constant of a population are given in Aksland (2005), based on integrated single-target echoes and their off-axis angles. Both types are based on particular assumptions and require echoes from a wide region of the main lobe, preferably out to the directions where the transmit and receive beam has dropped 20 dB. Therefore, their utility cannot be proved until they have been tried with real data. Notably, it is important to demonstrate whether the single-target echoes found in the echo signal satisfy the requirements for the estimators in Aksland (2005). For the purpose a new single-target detection routine is written, which extracts and integrates single-fish echoes within a wide region of the main lobe and over a wide range of echo strengths. Processing of the received echo signals from operating scientific echosounders is usually based on advanced computer programmes that have been developed over decades (see Korneliussen, 2004, and references therein).

The main purpose of this paper is to test the estimators for mean Echo Value Constant given in Aksland (2005), and for this it was necessary to write new programmes.

Material and methods

The file of acoustic raw data used in the analysis (provided by Egil Ona, IMR, Norway) was recorded with the

1054-3139/$32.00

SIMRAD EK 60 scientific echosounder system (split beam) onboard the Norwegian RV "G. O. Sars I". The file contained data from 3319 pings transmitted over a distance of 1.727 nautical miles on 5 April 2003. Speed was nearly constant between 9.9 and 10.1 knots, and the weather was good. The sound frequency was 38 kHz, and the pulse length 1.024 ms, although a small part of the recordings was with pulse length 0.512 ms. The signal-sampling interval was 0.256 ms for long pulse length, and 0.128 ms for short, giving roughly six signal readings over a single echo, including the tails. As the number of signal sample values over one pulse length was the same for both pulse lengths, these may be analysed in the same way, and can even be joined as one set of echoes. However, the shapes of the echoes, as well as the transmit pulses at full and half pulse length, were not quite the same, so it was decided to restrict the analyses here to the part of the transect with full pulse length.

The acoustic signals were converted from logarithmic to absolute values and multiplied with TVG (time-varied gain) functions. The signal levels were very low using the level described by SIMRAD, but as the method in this application is independent of signal level, it was decided to work with a level raised by 40 dB, simply because it then was easier to judge the dynamics of the echo signal from values written to a text file.

Routine to extract single-target echoes

A routine to extract the necessary quantities of integrated intensities and detection angles of single-fish echoes in a polar reference system was written. The theory of detecting the observation aspect angles with the split-beam system may be found in Reynisson (1999), and principles of single target-strength recognition in Ona and Barange (1999). This last description also holds for single-target recognition in the SIMRAD echosounder system software.

The routine for extracting single-target echoes is to some extent similar in principle to the SIMRAD routine, but there are some practical differences. Whereas the SIMRAD routine starts to search the echo-signal amplitude for parts that, in shape, satisfy some requirements for a single target, the present routine starts to search the alongship and athwartship angle signals for stable phase angles. The echo amplitude, with 40 log R TVG, is then searched for the presence of a single-target echo each time three successive angles with small variation were found in both angle signals. In general, the required number of similar angles will depend on the ratio between the pulse length and the sampling interval. The corresponding SIMRAD routine does not start with this test. The practical difference is that this routine extracts single targets of a wider range of echo strengths than the SIMRAD routine, which starts with imposition of a lower threshold for the echoes. The measure of phase-angle stability used in the present routine is the average absolute deviations between three successive angle values and their mean value, and the test value used for this quantity can be set.

Having found a possible single-target echo from analysing the phase angles, the current routine locates the peak value in the region of five successive amplitude values containing the stable angles as the central three. Then the first local minimum amplitude is found within, here, four amplitude readings to both sides of the peak. If these minimum values are sufficiently low relative to the peak value (a test value around 7% of the peak, but bigger for weak than for strong echoes, was used) and if none is found next to the peak, then the possible echo is subject to further calculations and test. No additional test for echo duration is applied.

The alongship and athwartship phase angles of the echo are first estimated as the mean value of the three most stable (as explained above) successive phase-angle values containing the site of the peak. This is done independently for the alongship and athwartship angles, after which the corresponding aspect (θ) and azimuth (φ) angles of the echo were computed. Next, the integrated intensity of the echo is computed as the sum of amplitude values between and including the echo minima on each side of the peak. Owing to the way these minimum locations are searched, they are never more than four amplitude readings from the peak.

The last test before accepting the echo as derived from a single target is based on the values of two indices referred to here as the alongship uncertainty index and the athwartship uncertainty index, respectively. These are defined as the average weighted absolute deviations between the actual angle values and the corresponding estimated angle for the echo over the region where the echo integral is computed. Two different multiplicative weights are used, one of which is the echo amplitude. This causes angle deviations at high echo amplitude to contribute much to the value of the uncertainty index. The other weight is a falling function of the distance to the peak. It is neutral (equal to one) near the peak, but it reduces the effect on the uncertainty index of large angle deviations in the echo tails, where large angle fluctuations are normal. The uncertainty index test accepts echoes with uncertainty indices below given limits that were set after inspecting the shapes of many echoes with different values of index. It was apparent that echoes with high values of uncertainty index were overlapping echoes.

Many versions of the complete routine for extracting single-target echoes were tried during programme development. The amplitudes, angles, and computed parameters for each echo that had passed one or more of the three described tests were written to files for inspection. Also, the shapes of many echoes were plotted. In this way, it was possible to adjust test parameters and to study their effects.

Computation of the estimators for mean Echo Value Constant

Routines for computing estimators (7)–(9) of Aksland (2005) have been derived. As the calibrated beam function

of the present survey was close to circular symmetrical, it was out of the question to attempt estimator (11). Developing routines for computing the first of these estimators was more demanding than deriving routines to compute the other estimators. Although it may be possible to compute Equation (7) without knowing the beam function of the transducer, the beam was known from sphere calibration in this application, and should be used.

For a near circular symmetrical beam, estimator (7) of Aksland (2005) may be written as

$$\widehat{\overline{\Psi}} = 2\pi \int_0^{\theta_c} \widehat{E}[\varsigma_{rb}(\theta)]\tan\theta \, d\theta, \tag{1}$$

where the integrand is assumed to be a constant function of φ, or that $\varsigma_{rb}(\theta)$ represents the average value at θ over all φ. $\widehat{E}[\varsigma_{rb}(\theta)]$ is the estimated expected integrated echo intensities of single-target echoes received at observational aspect angle θ. However, in accord with Aksland (2005), $E[\varsigma_{rb}(\theta)]$ will be referred to as the expected (beam-dependent) backscattering power at θ, where E is the expectation operator. The parametric model used here for the expected backscattering power is in fact a formula for the calibrated transmit–receive beam function, multiplied by a constant parameter. Although the backscattering power expectation may deviate from the beam shape at large aspect angles (likely 5° or more; see Figure 2 of Aksland, 2005), neglecting this here will have no practical effect on the estimator because of the narrow beam width.

If $B_{tr}(\theta)$ is an analytical formula for the transmit–receive beam function, then $E[\varsigma_{rb}(\theta)] = aB_{tr}(\theta)$ can be used for some value of parameter a. In this case, it is sufficient to estimate one parameter to compute Equation (1).

A formula used for the transmit–beam function of the split-beam transducer during calibration is given in Jech *et al.* (2005) and Reynisson (1999). The function is expressed in terms of the alongship and athwartship angles, and is a small-angle approximation. The split-beam transducer is quadratic, but has a circular symmetrical beam. Therefore, the circular symmetrical function is used here,

$$b_{tr}(\theta) = \left[\frac{2J_1(k\sin\theta)}{k\sin\theta}\right]^4,$$

where J_1 is the Bessel function of the first kind, and k is a parameter that determines the beam width. With $k = \pi D/\lambda$, $b_{tr}(\theta)$ is the theoretical transmit–receive beam function of a circular piston transducer of diameter D, transmitting sound with wavelength λ (Urick, 1983). These parameters are, however, not needed here because k is adjusted so that $b_{tr}(\theta)$ has the same half-power opening as the calibrated beam.

The following description makes use of the accurate approximation $\sin\theta \approx \theta$, which holds because of a narrow beam. The estimation procedure was based on the function $B_s(y) = (2J_1(y))/y$, where $y = k\theta$. It follows from the power-series expansion of the Bessel function that

$$B_s(y) = \sum_{n=0}^{\infty}(-1)^n \frac{y^{2n}}{(n+1)(n!)^2}. \tag{2}$$

This was used to compute values of B_s. With these symbols, the model used for the expected backscattering power is

$$E[\varsigma_{rb}(\theta)] = a[B_s(k\theta)]^4. \tag{3}$$

It is now possible to express Equation (1) in terms of k and an estimator $\widehat{a}$ of a. From Equations (1) and (3), $\widehat{\overline{\Psi}} = 2\pi \int_0^{\theta_c} \widehat{a}[B_s(k\theta)]^4 \tan\theta \, d\theta$. By also using the accurate approximation $\tan\theta \approx \theta$ and integrating with respect to $y = k\theta$, $dy = k\,d\theta$, we obtain

$$\widehat{\overline{\Psi}} = \widehat{a}\,\frac{2\pi}{k^2}\int_0^{1.92} y[B_s(y)]^4 dy, \tag{4}$$

where $y = 1.92$ is used for the upper integral limit. This includes exactly the whole main lobe of B_s. The integral is now over a unique function and therefore has a unique constant value. This is found by numerical integration to be **0.229276335203**. This number is emboldened to show that it is a mathematical constant independent of any variable parameters in applications. Graphs of the functions $[B_s(y)]^4$ and the integrand $y[B_s(y)]^4$ are shown in Figure 1. As the integral is computed numerically, the two approximations used to derive Equation (4) are not strictly necessary. In cases with wider beams, computations that do not use these approximations may be necessary.

The calibrated transmit beam had an opening angle at the −3 dB points of 7.045° on an average over the alongship and

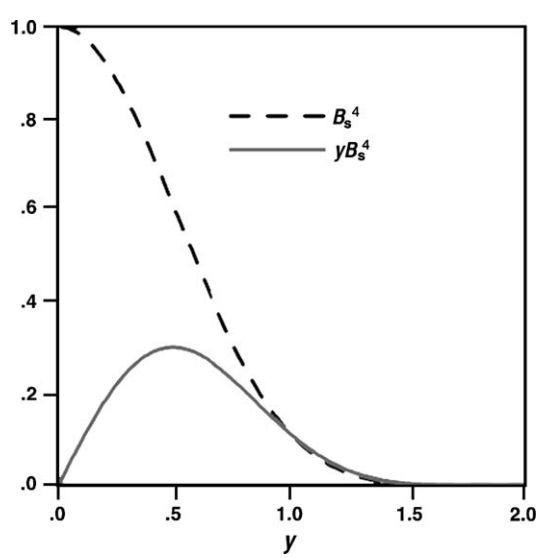

Figure 1. The beam and the integrand in Equation (4).

athwartship directions. This corresponds to $\theta = 3.5225°$, or 0.06148 radians. At this angle, B_s should be reduced to -1.5 dB, and this happens when $y = 0.8069$. Thus, $0.06148k = 0.8069$, which gives $k = 13.125$. These values lead to the following simple expressions for Equation (4):

$$\widehat{\overline{\Psi}} = \frac{\widehat{a}}{k^2}\,1.4406 = \widehat{a}\,0.008363. \tag{5}$$

Note that the first expression holds for all beams that satisfy the model used here, and the second holds for the particular calibrated beam in this study. The model for the calibrated transmit–receive beam is shown in Figure 2 as a function of θ, in degrees.

Now it remains to find an estimator for the parameter a. Let $w_1, \theta_1, w_2, \theta_2, \ldots, w_n, \theta_n$ be n observed, integrated, single-target echo intensities (backscattering powers) and associated observation aspect angles. It is then natural to estimate a by curvilinear regression. Using Equation (3), the sum of squared deviations between expected and observed backscattering powers is expressed as

$$Q_1(a) = \sum_{i=1}^{n} \left[w_i - aB_s^4(k\theta_i)\right]^2.$$

The value of a that minimizes Q_1 would be a least squares estimator of a. However, before choosing this, it would be useful to consider what is ultimately going to be estimated. This is the integral of the function $\theta a B_s^4(k\theta)$ with respect to θ. As $\theta_i a B_s^4(k\theta_i)$ is the expected value of $\theta_i w_i$, it is better to base the least square on this and to use

$$Q(a) = \sum_{i=1}^{n} \theta_i^2 [w_i - aB_s^4(k\theta_i)]^2. \tag{6}$$

An expression for the value of a that minimizes Q is found by the standard method of equating $\partial Q/\partial a$ to zero, and yields

$$\widehat{a} = \frac{\sum_{i=1}^{n} \theta_i^2 w_i B_s^4(k\theta_i)}{\sum_{i=1}^{n} \theta_i^2 B_s^8(k\theta_i)}. \tag{7}$$

The estimator (7) can now be used in Equation (5) to compute an estimate of the mean Echo Value Constant.

Because the terms of Q having low or high values of θ_i are very small, the estimator $\widehat{a}$ will not be sensitive towards single-target echo values observed at small or high aspect angles. This is an advantage, because echoes at high values of θ are likely to be biased as a consequence of both observation error and the loss of many echoes. However, if the echo data are not biased in any region of the beam and the model used for the expected backscattering power is good over large regions of θ, Q_1 may be better than Q. However, because Q is most sensitive to the echo data only at values of θ where the integrand in Equation (3) is high, this will also be advantageous if the model is unable to describe the expected backscattering power correctly over a wide region of the main lobe. The beam model used here may deviate from the true beam shape, particularly when $\theta > 6°$.

Estimators (8) and (9) in Aksland (2005) are readily computed directly from their formulae. The second estimator is given in Results as Equation (8). The question is, however, whether the assumptions behind the estimators are properly fulfilled. This is most doubtful for Equation (8), because Equation (8) requires the observation of a number of single-target echoes having the properties of a random sample from the probability distribution (13) in Aksland (2005), out to around -20 dB of the transmit–receive main lobe. There are, however, different methods to modify Equation (8) so that it can be used without bias of significance when many weak echoes far out in the beam cannot be observed.

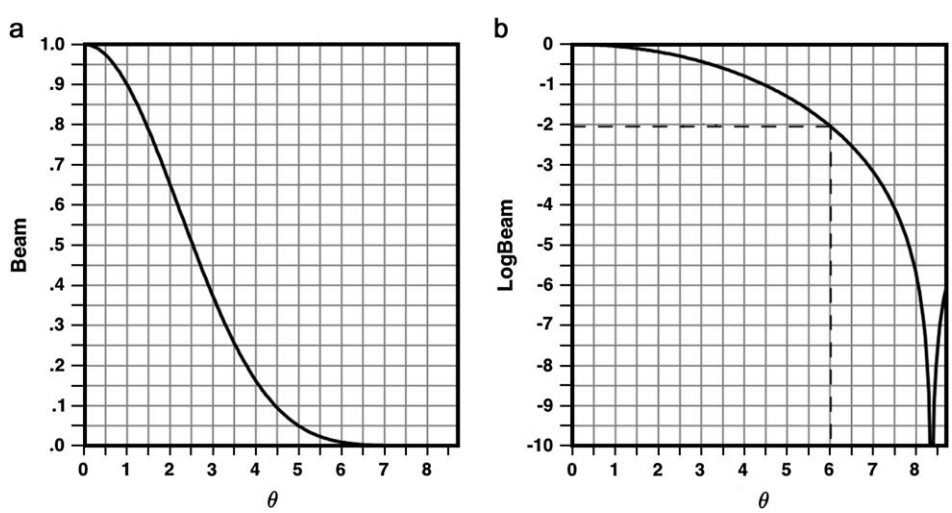

Figure 2. The model used for the φ-averaged calibrated transmit–receive beam on (a) an absolute and (b) a logarithmic scale. The beam falls 20 dB when θ is around 6°.

One idea is to estimate the ratio, as a function of θ, between the theoretical and observed distribution of observation aspects, and to use this ratio as weights for the terms in the sum of estimator (8). This is not tried in this paper, but the following idea is. Estimator (8) is computed for a set of angles in small steps from zero to θ_c or beyond instead of only for θ_c. If Equation (8) is not biased because all single-target echoes are observed, these values as a function of θ are expected to follow the Echo Value. Presuming that the expected beam-independent backscattering power distribution is a constant function of θ (likely for small angles), it should be possible to compare this estimated echo value with a scalable echo value of a sphere computed for the calibrated beam.

If a theoretical echo value can be scaled (multiplied by a constant) to join the estimated echo value over some range of θ-values, typically from zero out to some angle less than θ_c, it can be expected that the true echo value for the fish can be followed also for angles where the estimated echo value is biased. The mean Echo Value Constant may then be estimated from the scaled theoretical echo value. This method is tried in this paper.

Echo-signal integration

The integrator values of the signal with 20 log R TVG were computed for each ping simply as the sum of the amplitude readings. This is in accord with the way each single-target echo was integrated. Each ping was integrated from a depth slightly below 40 m and to the bottom, because this interval contained all NE Arctic cod (*Gadus morhua*) echoes. To avoid integration of any part of the bottom echo, integration stopped at the first local signal minimum of low amplitude above the bottom echo.

It was out of the question to interpolate and integrate integrator values over any area, because the file of raw data contained the acoustic signal from a part of one straight transect only. Instead, the integrator values were averaged over pings that may be multiplied by the length of the actual transect. As the cruising speed was constant, this is the same as integrating the integrator value as a function of each ping with respect to distance sailed. This quantity must then be multiplied by a distance perpendicular to the transect to obtain a quantity that has the unit of echo abundance. By dividing this echo abundance by the estimated mean Echo Value Constant, an estimate of the number of fish below the actual area is obtained. In particular, using the ping-averaged, integrator values multiplied by 1 m^2, an estimate of the average fish density in number of fish per m^2 under the transect is obtained. The mean fish density per m^2 is estimated in this manuscript.

Results

Typical echograms from the recordings in the file of raw data are shown in Figure 3. Pings 658−1018 were with half pulse length and signal-sampling interval, and are not shown. The remaining, pings 1−657 and 1019−3319, were with full pulse length (1.024 ms), and are used in the analysis.

The depth difference between the horizontal division lines is 10 m. As seen, the depth distribution of cod is mainly below 50 m, and most cod seem to stay high enough off the bottom to be correctly integrated. In some parts of the registration (Figure 3b), it is possible to see echoes from smaller organisms mixed in between the cod echoes. It would have been possible to exclude many of these echoes from the echo-integration based on where they are on

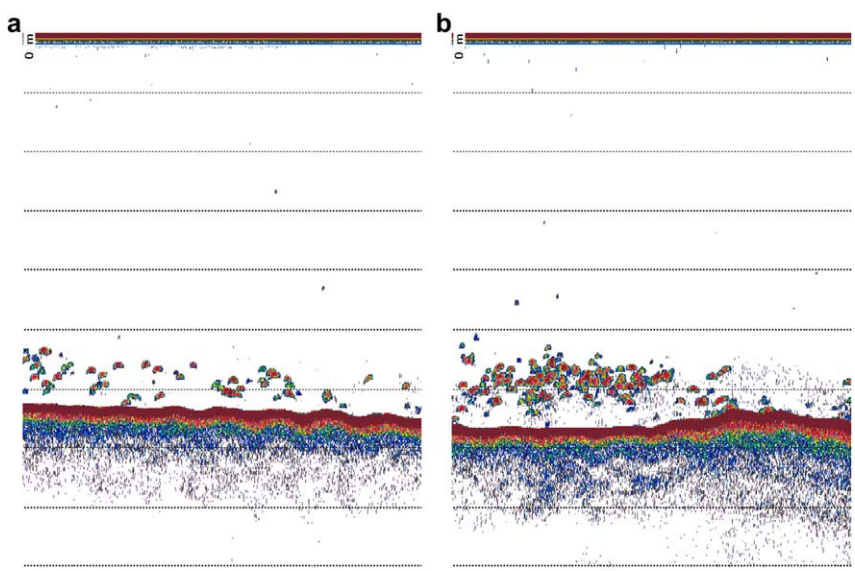

Figure 3. Echograms generated from the file of raw data used in the analysis herein.

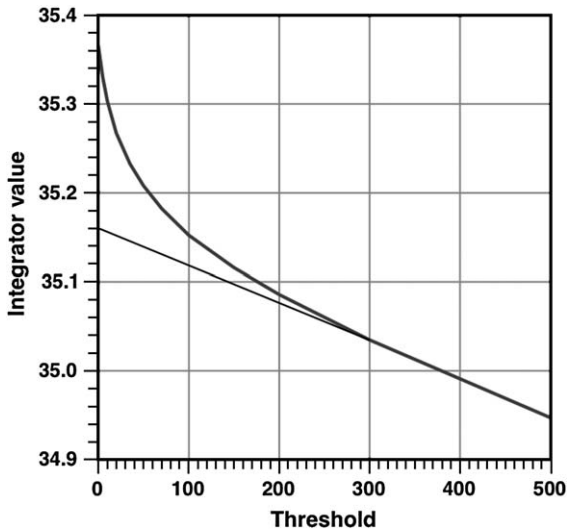

Figure 4. Mean integrator value per ping as a function of 40 log *R* TVG threshold. The value where the straight line intersects the vertical axis is used as the mean integrator value. The 20 log *R* TVG signal was integrated when the 40 log *R* signal was above the threshold.

the echogram, but to save programming time this was not given priority. After all, the integrator value of the cod echoes was judged to be an absolutely dominant part. Some echoes from small organisms can be removed by applying a threshold, but this may also exclude some weak parts of the cod signal.

Echo-integration

Echo-integration was repeated with the use of different threshold levels. The fall in the mean integrator value per ping is shown in Figure 4, and based on the figure, the mean integrator value is set at 35.16. This is where some tangent at the lower part of the curve cuts the *y*-axis. It is then likely that the contribution by noise and many small echoes from plankton is removed without reducing the integrator value of cod echoes. The steep slope at small thresholds indicates that a threshold removes something that is almost everywhere, i.e. noise plus weak plankton echoes. When this is finished, the slope is flatter, and it is then likely that contributions from cod are removed, because many weak echoes from cod have peak values in the order of a few hundred in terms of the signal intensity level worked with in this paper. Note that the proposed reduction in the mean integrator value is about 0.4%. The variation of the integrator values along the transect is shown in Figure 5, together with the bottom contour and how far above the seabed the echo-integration stopped.

Extraction of single-target echoes

Extraction of single-target echoes with full pulse length resulted in roughly 3000 accepted echoes, depending on the level of angle stability used in the single-target recognition routine. When the angle-stability test was used with different values of allowed angle variation, the number of accepted echoes increased with increasing value, but it levelled off when the allowed angle variation was large. This showed that the other tests, on echo shape and uncertainty indices, limited the number of accepted echoes when the first test was too open. Based on this study, it was decided to use test levels that accepted a total of 2960 echoes with full pulse length from depths below 41.5 m (depth index 220). The maximal allowed angle stability used was 1° average angle variation over the three most even angles containing the echo peak. There may be some good echoes that were not detected at all with this test setting, but for those, estimation of detection angles would be rather imprecise. Figure 6 shows some echoes of different quality and strength together with the angle signals. Echo a is rejected because the first local minimum to the right of (below) the peak is too high relative to the peak. Echo b is rejected

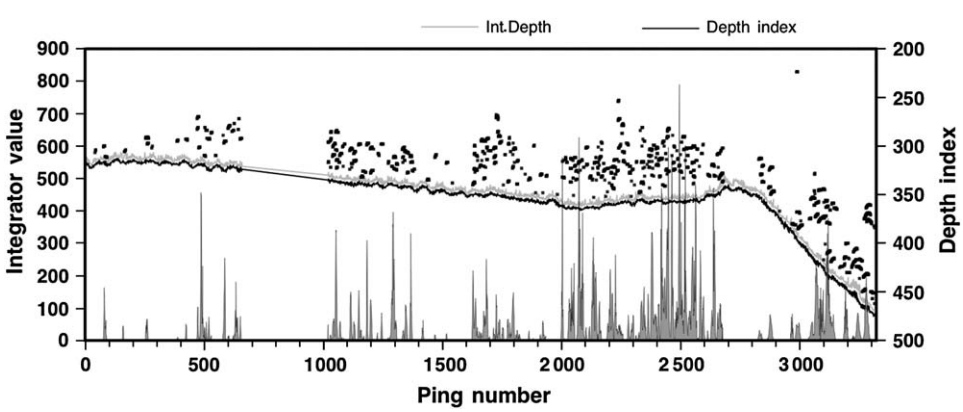

Figure 5. Integrator value and indices for depth and integrator depth as a function of ping number, and the positions of the extracted single-cod echoes used to estimate the Echo Value Constant. The empty part around ping number 800 is excluded because of the use of a half pulse length.

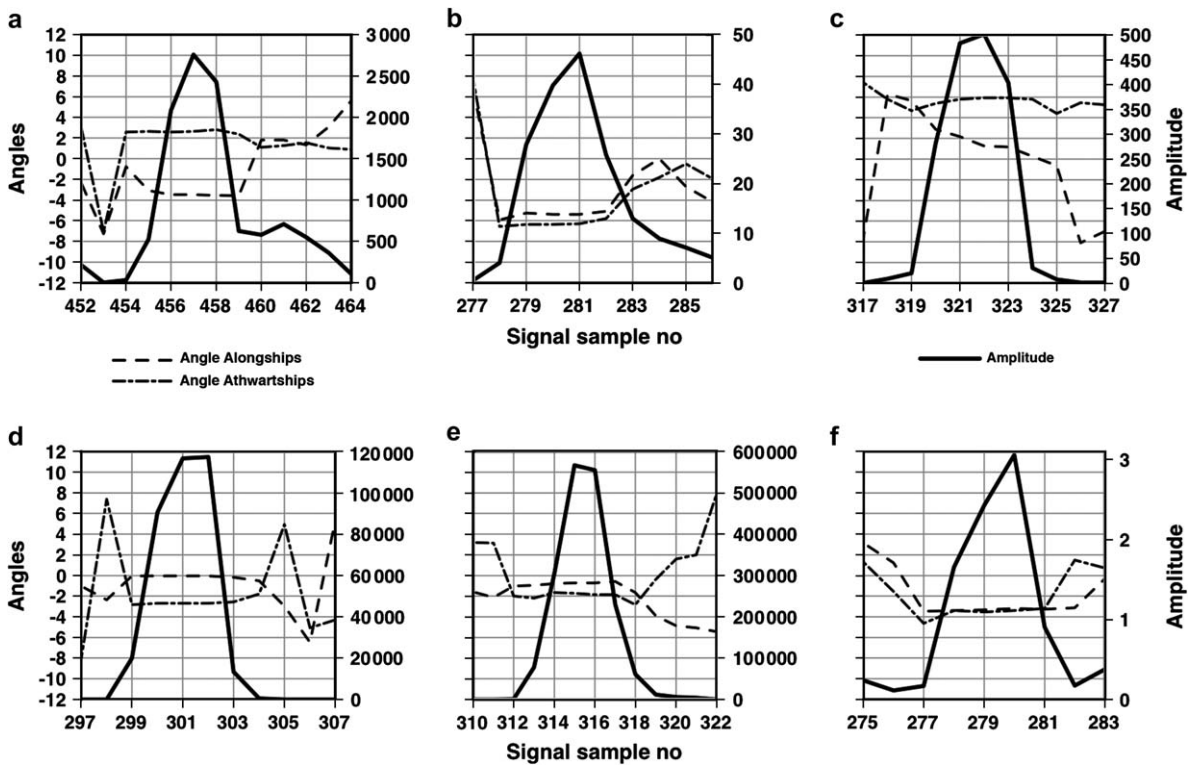

Figure 6. (a–c) Echoes not accepted; (d–f) accepted echoes. See text for details.

because the uncertainty indices are too high, and echo c fails unless the angle-stability test is rather open, because the variation in the alongship angle is too large. If the large angle variation does not reject this echo, it is rejected by the uncertainty index test.

Of the accepted echoes, echo d is an example of a good echo with very stable angles, and echo e is a very strong echo (in fact the strongest observed). Finally, echo f is a very weak, but at the same time a reasonably good, echo. It is natural to suspect that echo e, because of its extreme strength, might be a perfect overlap between two strong echoes. This was investigated by studying the neighbouring pings. If two echoes overlap perfectly in one ping, it is likely that they do not overlap in some other nearby ping where they also are observed. From this, it was clear that echo e overlapped with a much weaker echo in the right tail. This would not bias its integrated intensity significantly because echoes are never integrated over more than four amplitude values away from the peak.

Scatterplots of the logarithms (log 10) of the integrated intensities (BSP) against their aspect angles of all accepted echoes with long pulse length are shown in Figure 7. The backscattering powers (integrated single-echo intensities) are damped by the beam function. The densest and upper parts of the scatterplots are obviously derived from cod, whereas the more scattered points below those parts are from smaller organisms, or in part from cod in the first side lobe, which is roughly 35 dB weaker than the main lobe. It is surprising that this routine has extracted echoes with a dynamic range of about 60 dB in backscattering power.

Estimates of mean Echo Value Constant and mean fish density

Before using these echoes to estimate the mean Echo Value Constant for cod, a border between cod echoes and echoes

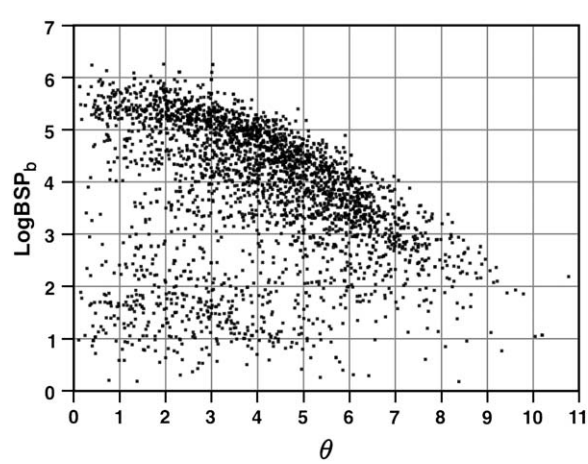

Figure 7. Observed distributions on a logarithmic scale of the beam-dependent, backscattering power of all echoes with full pulse length as a function of θ in degrees.

from smaller organisms has to be determined. Figure 2 of Aksland (2005) shows simulated target-strength distributions for narrow length groups of fish. As target strength is proportional to backscattering power, echo strengths from large cod of roughly equal size can be expected over a range of about, or slightly more than, 20 dB at the present frequency of 38 kHz for fixed values of θ. As there is obviously a spread in cod sizes, cod echo strengths are here assumed to show a variation over at least 25 dB for fixed θ. Before using the echoes, they must pass a test of echo strength depending on θ, where echoes slightly more than $\sim$25 dB weaker than the strongest echoes for the actual value of θ are excluded. A θ-dependent threshold proportional to the calibrated beam function was used.

Figure 7 indicates that the beam model displayed in Figure 2 is not correct at large angles around the minimum between the main and first side lobes. However, echoes from far out in the main lobe are also likely to have errors in backscattering power, or detection aspect, or both. It was therefore decided to use echoes with aspects $<6°$ to estimate the Echo Value Constant. In the following analyses, these restrictions have been made. Another requirement that should be looked at is whether the selected echoes can be considered to derive from a unique backscattering power distribution over the entire transect. Figure 8 shows how the beam-independent backscattering powers are distributed over the transect (ping numbers).

The levels of echo strength in local concentrations of echoes show variations along a transect. Although the θ-dependent threshold has removed weak echoes in Figure 8 likely to have come from smaller individuals of other species, or from the side lobes, it is unlikely that each echo displayed in Figure 8 is from cod. A further removal based on echo strengths of echoes likely to have come from other species seems difficult, but the groups around ping numbers 270 and 2840 are suspicious.

As it seems difficult to find some stratification of echoes based on local backscattering powers, it was decided to use all echoes to estimate one mean Echo Value Constant. Conditions for doing this without generating a biased abundance estimate are considered in Discussion.

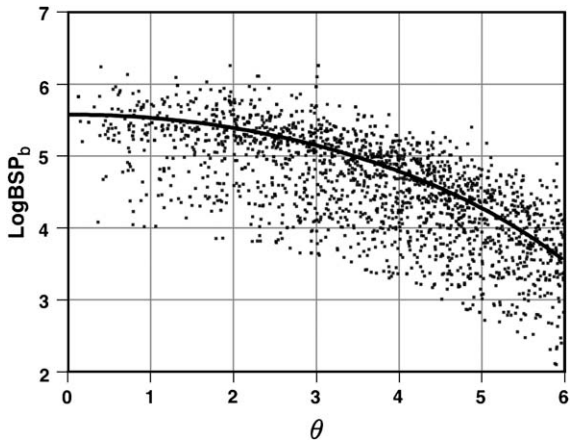

Figure 9. The echoes in Figure 7 limited by θ less than 6° and a θ-dependent threshold of 4 at the acoustic axis, and the estimated mean backscattering power function for cod (see estimator (3)) displayed on a logarithmic scale.

Figure 9 shows that function (2) used for the beam shape seems to fit the single echoes satisfactorily at detection angles up to 6°. By using the selected echoes, estimates of estimators (7) and (5) were $\widehat{a} = 376\,423$ and $\widehat{\overline{\Psi}} = 3148$, respectively. Furthermore, by dividing the mean integrator value from Figure 4 by $\widehat{\overline{\Psi}}$, an estimate for the mean cod density under the transect observed with long pulse length is obtained as mean cod density $= 0.01117\ \mathrm{m}^{-2}$, or about 45 cod per acre.

It is not easy to set an appropriate level for the single-echo threshold, and attempts were made to run the computations with the θ-dependent threshold increased and decreased by 1 dB, respectively. This showed that the estimate changed about 1%. Setting of an echo threshold is, therefore, not very critical to this application. The sensitivity towards

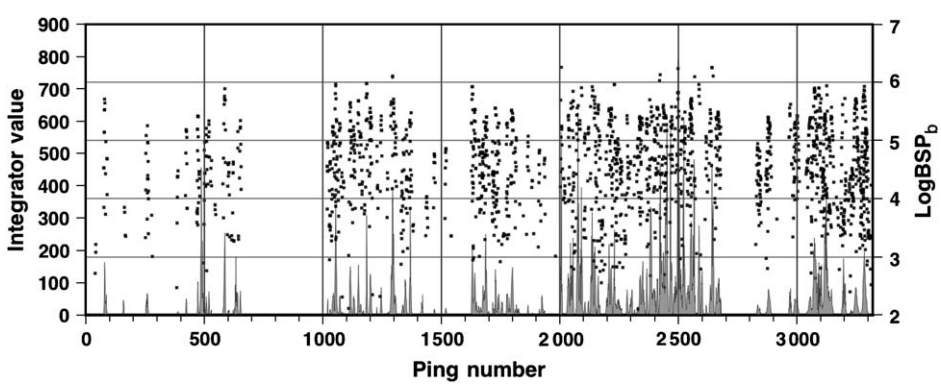

Figure 8. Selected beam-independent backscattering power (BSP) on a logarithmic scale for single NE Arctic cod along the transect, together with 20 log R TVG integrator values.

changes in echo threshold depends on the fraction of echoes removed from or added to the echoes used.

Fulfilment of the conditions for using estimator (9) of Aksland (2005) also needs to be investigated. This estimator has the form

$$\widehat{\Psi}'_3 = \frac{\pi \tan^2 \theta_c}{n} \sum_1^n w_i \cos^2 \theta_i, \quad (8)$$

where $(w_i, \theta_i) \quad i = 1, 2, \ldots, n$ are the backscattering powers and detection angles of n single-target echoes observed out to angle θ_c, an angle where the transmit−receive beam has dropped about 20 dB or more. Derivation of this estimator requires that the empirical distribution of the detection angles follows the theoretical distribution (13) and density (14) of Aksland (2005). This density has the form

$$f(\theta|\Theta \le \theta') = \frac{2}{\tan^2 \theta'} \frac{\tan \theta}{\cos^2 \theta}, \quad \text{for } 0 \le \theta \le \theta', \quad (9)$$

where θ' should not be less than θ_c. For small angles where $\tan \theta \approx \theta$ and $\cos \theta \approx 1$, this probability density increases approximately linearly with θ.

A histogram of the observation aspects of the echoes displayed in Figure 9 is shown in Figure 10a. The aspect-angle distribution seems to follow the theoretical probability density up to roughly 4.5°. This is not enough for estimator (8), which here requires echoes up to 6°. Modification of estimator (8) described in Material and Methods is therefore applied by computing Equation (8) for each half-degree angle up to 10°. This function is denoted as EVe, meaning the estimated mean Echo Value. Both EVe and a corresponding theoretical Echo Value, EVt, of a sphere were plotted in the same reference system, and EVt was scaled until it became concurrent with EVe for a range of small angles. EVt should then converge to an estimate of mean Echo Value Constant at angles of 6° and above. The success of this method in this study is shown in Figure 11.

As the mean Echo Value Constant was estimated to be 3148 by the other method, Figure 11 seems to agree satisfactorily. EVe starts to overestimate mean Echo Value at angles around 4°, or just where the empirical aspect-angle histogram in Figure 10a fails to have a shape corresponding to the theoretical probability density (9).

Estimator (8) of Aksland (2005) is a version of Equation (8) here that accounts for missing echoes far out in the beam. Although the assumptions for this estimator may not here be completely fulfilled, the version should, nevertheless, be tried. It takes the value 3064° that is not far from the other estimates. This estimator may give good estimates provided θ_0 is not small relative to θ_c.

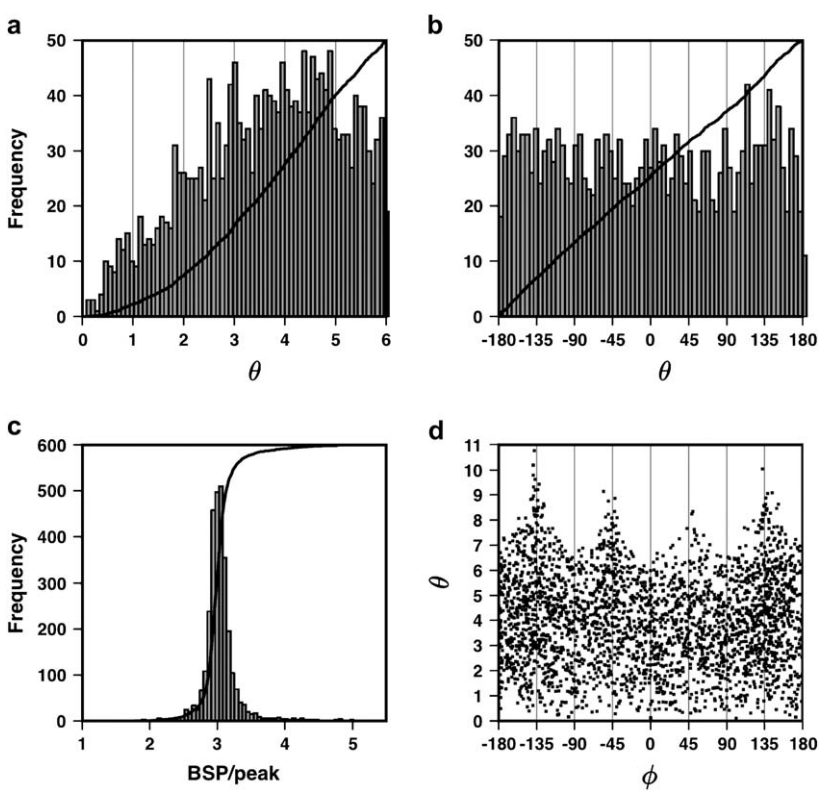

Figure 10. Observed distribution of the echoes represented in Figure 9 using (a) aspect angles and (b) azimuth angles, (c) the ratio between the backscattering power and the peak value of all echoes represented in Figure 7, and (d) a scatterplot of the bivariate distribution of all aspect and azimuth angles of the echoes under (c).

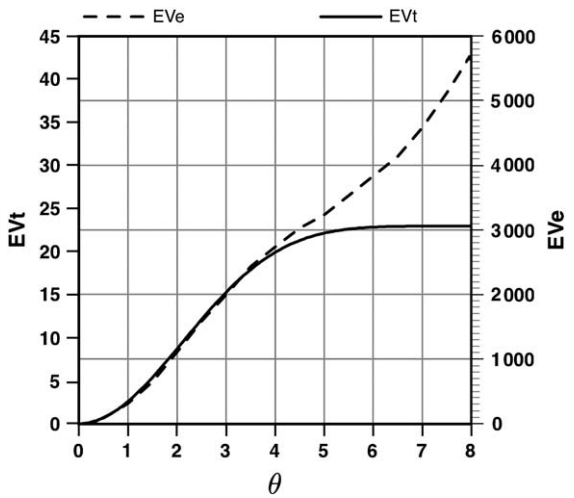

Figure 11. Theoretical and estimated Echo Value adjusted almost to coincide at angles less than 4°.

Fish-density estimates by the classical echo-integration method

The same file of raw data was used by Egil Ona of IMR, Norway, to compute fish-density estimates by means of standard programmes for echo-integration. The mean backscattering cross-section was not estimated from catch samples because no cod samples were taken close to the transect analysed. Moreover, the output level of EK60 had not been calibrated, because it was the first time it had been used on an experimental basis on a research vessel by the Institute of Marine Research, Norway. The mean backscattering cross-section of cod was therefore estimated from *in situ* target-strength measurements (see Ona and Barange, 1999).

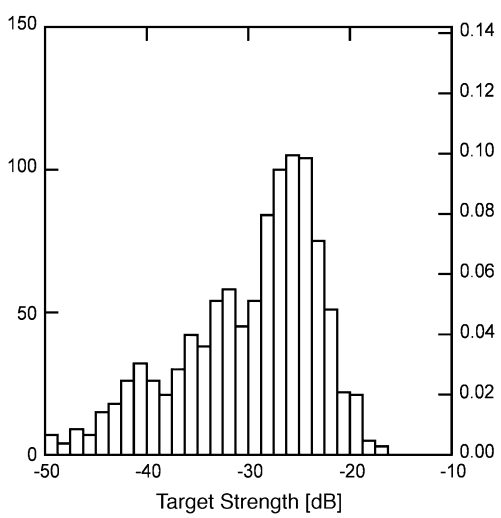

Figure 12. Target-strength distribution observed between 40 m deep and the seabed, cut off at −50 dB. The units on the left *y*-axis are the number of echoes, and on the right *y*-axis the echo frequency.

Table 1. *In situ* estimated mean backscattering cross-section at different levels of target-strength threshold for NE Arctic cod.

Target-strength threshold (dB)	Mean backscattering cross-section (m^2)
−50	0.029317
−45	0.032354
−40	0.036009

Mean integrator values for depths below 40 m within intervals of 100 pings were computed over the complete transect. *In situ* target-strength measurements were also recorded at the same depths over the whole transect and used to estimate the average backscattering cross-section of the targets entering the beam. The resulting target-strength distribution is shown in Figure 12. This target-strength distribution gave the estimates in Table 1 of the mean backscattering cross-section at three values of the single-echo threshold. Dividing the average area-backscattering strength (s_A) on the mean backscattering cross-section gives an estimate of the mean fish density per square nautical mile.

To obtain an average fish-density estimate corresponding to the estimate based on Equation (5), the average s_A values within ping numbers 1−600 plus ping numbers 1001−3319 was computed. This is not exactly the set of pings with full pulse length, but the small difference that exists is not likely to be important. The average s_A over this region is 1251.96 m^2 nautical $mile^{-2}$. This gives an estimated fish density of 0.01128 per m^2 when a −45 dB echo threshold is used, 1% greater than the alternative estimate based on Equation (5). However, it is likely that the −45 dB threshold represents a slightly lower threshold than that used to compute the alternative estimate, judging from Figures 9 and 12. The classical estimate based on a −40 dB echo threshold is 0.01014 fish per m^2, i.e. less than the alternative estimate. However, when the alternative estimator (5) is recalculated with a 1 dB lower single-echo threshold, it takes the value to 0.01128 per m^2, the same as the classical

Table 2. Estimates of mean Echo Value Constant and corresponding mean NE Arctic cod density by different estimators of the alternative echo-integration method. The estimates in parenthesis are based on reading of a value on the right-hand *y*-axis of Figure 11.

Estimator	Echo value constant	Cod density per m^2
Equation (5)	3 148	0.01117
Figure 11	(3 060)	(0.01149)
Estimator (8) of Aksland (2005)	3 064	0.01148
Estimator (5), with a 1 dB reduced threshold	3 179	0.01128

Table 3. Estimates of mean NE Arctic cod density by the classical echo-integration method, using *in situ* target-strength estimation for two values of target-strength threshold.

Target-strength threshold (dB)	Cod density per m^2
−45	0.01128
−40	0.01014

estimate with a −45 dB target-strength threshold. The range of echo strengths used to compute these estimates may, however, still be slightly different.

Tables 2 and 3 summarize the computed estimates. The result for a −50 dB threshold is not displayed in Table 3, because it is likely that the local mode on the extreme left in the target-strength distribution of Figure 12 contains many echoes from organisms smaller than cod.

Discussion

It is not surprising that the alternative and classical *in situ* method yields close estimates to those derived here. The methods are based on similar principles, notably that this method is based on a calibrated beam and the assumption of constant beam-independent backscattering power. This corresponds to the classical method's implicit assumption that the mean backscattering cross-section is independent of the detection angle, which requires use of sufficiently narrow beams. Both methods are also independent of the actual output level of the echosounder, as long as it is stable, a property that is not true when the mean backscattering cross-section is estimated from catch samples. The alternative estimates show a difference of between 2% and 3%, and the classical (−45 dB threshold) estimate has an intermediate value.

It is interesting that estimator (8) of Aksland (2005) is independent of the beam model; it is derived under the assumption that a θ-independent threshold limits the number of echoes far out in the beam. This is certainly not the case in the current application, but the process that limits the echoes used here certainly affects weak echoes more than strong echoes.

Estimator (8) of this work is also independent of a beam model, but it depends on the beam model through computation of the theoretical Echo Value. It may be possible to develop other modifications of the estimator that explicitly use deviations between the empirical and theoretical aspect-angle distribution. This estimator will then be independent of a beam model. A natural continuation of the development of an alternative echo-integrating method would be to derive and test this modified estimator.

Integration of a 20 log R TVG signal is straightforward in principle, but requires setting of a proper value of the integrator threshold. Furthermore, integration near the bottom echo for registrations close to the seabed may sometimes be a challenge both technically and in data analysis terms. The use of an integrator threshold in this application to remove the contribution from noise, plankton, and small fish seems to be successful, but there may be a small bias in the computed mean integrator value attributable to the loss of some fish echoes that partly overlap with the seabed echo. The presence of some such echoes are apparent from inspection of the echo signal. The routine to extract single-target echoes in this application seemed to work satisfactorily, but because the analysed acoustic data consisted mainly of resolved echoes, more challenging, as well as laboratory controlled, tests are necessary to draw general conclusions.

The calculation of integrated single-echo intensities seemed to work satisfactorily, but a relative error that increases with the weakness of an echo is likely. The data analysed here had a very good signal-to-noise ratio, and it is likely that errors caused by a higher noise value will be more serious for measuring integrated intensity than for the peak value. However, in such cases, it should be possible to estimate the integrated intensity from the peak value by means of a ratio computed from the strong echoes.

The result in Figure 10c seems strange. The largest aspect detection angles are only observed around azimuth angles of ±45 and ±135°. This is obviously due to limitations with the equipment, but it can also in part be caused by a non-circular beam shape far out in the main lobe. An objective, therefore, should be to increase the precision and quality in the angle signals of weak echoes and echoes from far out in the main lobe. Another surprise was the apparent variation in the shapes of good echoes when studying the shapes of many single-target echoes. Figure 10c illustrates this by showing significant variation in the ratio between backscattering power (BSP) and peak value. Variable shapes of the echoes are not the only cause of the variance of this distribution. Another cause is errors in the recorded peak values caused by the long signal-sampling interval relative to pulse length. In this case the true peaks are seldom hit. This may affect target-strength measurements as well as abundance estimation (Jech *et al.*, 2005). There may also be variations in computed backscattering power (the sum over amplitude values) caused by the long signal-sampling interval, but this will be smaller than the corresponding error in the peak value detected. Despite this, it is the real variation in the echo shapes that really makes it difficult to establish models for the echo shape for use in better determination of echo parameters or in recreating the shapes of the members of partly overlapping echoes.

The echoes are slimmer than the transmit pulse. With full pulse length, the ratio between integrated pulse intensity and peak value is 3.30 for the transmit pulse and a mean of 2.99 for the echoes. The corresponding values for a short pulse length are 3.14 and 2.88. The alternative echo-integration method used here performs independent of these ratios when they are not changed within a survey, but those ratios do have to be considered with the conventional approach.

With the classical method, the mean backscattering cross-section estimate is based on all pings, because of difficulties in applying the standard programme on two separated intervals, whereas mean Echo Value Constant estimates are based on just full pulse-length pings. This is likely to have a small effect, however, because the standard programme automatically compensates for changes in echosounder settings, and also because the mean single-fish echo strengths in the small set of pings with half pulse length seemed to be fairly similar to those with the full pulse length.

The problem of establishing a reliable conversion of echo integrator outputs to fish abundance has existed since the first use of echosounders to detect the presence of fish. The extended use of models for mean backscattering cross-section of fish as a function of species, size, and other body characteristics obtained from catch samples is still the standard method to obtain fish-density estimates acoustically, despite the existence of methods based on *in situ* measurements of target strength. *In situ* methods, including the estimators used in this paper, are supposed to work under varying distributions of target strength within the same population. This is an advantage over the standard method. However, *in situ* methods do not work when the echo signals consist mainly of overlapping echoes, and have sources of bias not shared by the standard method. These biases will occur when the single-target echoes used are not representative of all echoes from the target population being integrated. The sources of bias with *in situ* methods may be classified into three types: (i) acceptance of overlapping echoes as single-target echoes; (ii) acceptance of false echoes (echoes from fish not belonging to the target population); and (iii) the recorded echoes are good and real single-target echoes, but the sample is skewed relative to representative echoes from the target population.

Occurrence of the first type of bias depends on the quality of the single-target detection routine in use. Weaknesses with an earlier version of SIMRAD's EK 500 routine to isolate echoes from single fish are reported by Soule *et al.* (1995). Use of *in situ* single-target echoes to estimate target-strength probability distribution began with use of the Craig and Forbes method for single-beam systems. This was replaced with Clay's beam-deconvolution method (Clay, 1983). When dual beam systems came into use, it was still important to measure target strength *in situ* when fish density was low enough for overlapping echoes not to occur. Research to determine the maximum mean number of fish per reverberation volume without overestimating mean target strength was conducted (Gauthier and Rose, 2001). The problem of accepting overlapping echoes is also analysed by Ona and Barange (1999). However, the use of good single-target detectors will limit acceptance of overlapping echoes even when applied over local dense concentrations of fish. New techniques to discover overlapping echoes by utilizing more than one transducer (Demer *et al.*, 1999) may perhaps be developed to eliminate the inclusion of almost all overlapping echoes. To avoid overlapping echoes is not, in my opinion, the correct objective for single-target detection routines. This is because the echo signal contains numerous weak echoes from plankton and other small particles, as well as many more echoes from the low sensitivity portion of the beam than from the central high sensitivity portion. This means that the detected echoes usually overlap with more or less weaker echoes. A more appropriate objective for single-target detectors would therefore be to extract echoes from single fish of which the target strength, or the backscattering power, may be measured without significant error. It is only when two or more echoes of comparable strength overlap perfectly that this is not fulfilled.

The second type of bias is not easy to avoid when species are mixed. A common type of false echo is weak echoes from plankton and other (e.g. prey) species that are often mixed with fish of the target population. Approaches to reduce the bias of *in situ* methods caused by false weak echoes include the use of a suitable threshold for single-target echoes. It is, however, not easy to set a value for the threshold that eliminates this bias if the two groups of echoes overlap in the scatterplot, as in Figure 7, or in the target-strength distribution. The work conducted here illustrates this here by selecting a single-echo threshold that accepts some of the unwanted echoes and excludes some of those wanted. Another way of excluding unwanted echoes would be to identify them as being in areas of the echograms that will not be used at all. This is seen from the echogram in Figure 3b. Of course, an echogram signal threshold low enough to make the false echoes visible is necessary for this approach to be successful. A promising future tool to reject echoes from non-target fish is the use of multi-frequency systems that can identify echoes to species or categories of species (Korneliussen and Ona, 2003; Logerwell and Wilson, 2004).

The third type of biased single-target echoes is likely to be the most difficult to evaluate. As single-target detection routines reject echoes that do not satisfy every test of the routine, a selective process collects single-echo samples. In general, fish that generate resolved echoes in dense concentrations are likely to be special. This means that even if it is possible to develop reliable single-target detection routines for use when the echo signal consists of a large fraction of overlapping echoes, the collected echo samples may not be representative of the target individuals being surveyed.

It is important to be aware of the special circumstances that can cause bias when applying the alternative echo-integration method. This is not the same for the different types of estimators used here. The estimator given by estimators (5) and (7) requires that the single-target echoes used have a backscattering power distribution with a mean value, as a function of θ, that represents the expected mean backscattering power distribution of the group of fish to be estimated. The most likely source for biasing the observed distribution of backscattering powers is that

the probability of detecting a single target decreases with its weakness. This effect is apparently present and is the likely cause for observing considerable fewer echoes than expected far out in the main lobe, as shown in Figure 10a. A likely reason for this is that weak echoes are far more numerous than strong echoes and therefore overlap more often, and their angle signals are more disturbed because of their weakness. The strong echoes, of course, also overlap equally often with weak echoes, but this will usually not affect their angle signals or echo strengths significantly. The effect of a reduced number of detected weak echoes will be a positive bias for the mean backscattering power of echoes at the largest aspect angles used in the estimator, but to have a significant effect on the estimate, it must be biased in the region of the angles where the integrand in Figure 1 is high. This is roughly within the -10 dB limit of the transmit–receive beam, or in the case of this application, when $\theta < 4.5°$. The danger of this type of bias is greater with wider actual backscattering power, or with wider target-strength distribution. This distribution is, of course, wide when it represents a group of fish, or organisms, of considerably different sizes, but also for active fish with wide body-aspect-angle distribution.

It is not likely that the effects discussed here have caused serious bias in the estimates computed from Equations (5) and (7), because the observed detection aspect distributions follow roughly the shape of the corresponding theoretical distribution up to roughly 4.5° (Figure 10a). Estimator (8) or (9) of Aksland (2005) is sensitive to the observed distribution of detection angles. If this distribution is not in accord with the theoretical density (9), or (13) and (14) of Aksland (2005), the estimate will be biased. Estimators (5) and (7) are not in that degree sensitive to deviations in the distribution of detection angles. The normal type of deviation of an observed relative to a theoretical detection angle distribution is a strong reduction of the number of observed echoes at large detection angles, and this means that estimator (8) cannot be recommended in its original form. As shown in Figure 11, however, modifications of this estimator may work if the observed angle distribution follows the shape of the theoretical up to some angle that is not small relative to the angle where the Echo Value Constant is reached.

The problem of varying target strength, or backscattering power distribution along the transect, still needs to be discussed. Such variation is apparent in Figure 8. If the backscattering power distribution seems to be stable within much of the transect, but still different between some parts, stratification of the estimation method is worthwhile. However, if there are apparently random, non-systematic short-distance variations in the level of backscattering powers, as in Figure 8, stratification is not practical. Such variations may be caused by the presence of many small concentrations of fish of differing individual size, or different activity levels. If the fraction of the detected single-target echoes in the acoustic signals from such local groups is equal, then the use of all echoes in an estimator of the mean Echo Value Constant is likely to give an unbiased estimate.

One situation where this is fulfilled would be when the acoustic signals do not contain overlapping echoes of significance. Another is when the average fish density is the same within the local groups of different fish at similar depths. Such a situation is unlikely, because fish have a tendency to adjust their density to values that decrease with increasing fish size. This means that when an insignificant fraction of the echoes overlap, joining echoes from apparently differing backscattering power distributions to estimate the mean Echo Value Constant is likely to lead to a biased estimate. In the application herein, only a small fraction of overlapping echoes from cod occurred in the acoustic signals. This means that the effects discussed here will only slightly bias the estimates of the mean Echo Value Constants.

Another characteristic with *in situ* methods is that the number of extracted single-target echoes is strongly dependent on the range. Provided that all echoes are resolved, the number of echoes received from different ranges, or depths, of a scattering layer of constant fish density will be proportional to the squared range because of the geometric spread of the beam. This can be a serious source of bias in estimates of mean scattering cross-section, or Echo Value Constants, if the upper and lower part of a scattering layer consists of fish of different size, or if there are different target strengths for other reasons. The effect of oversampling deeper parts of layers is stronger the closer the transducer is to the top of the layer, and this has to be considered when using towed transducers to collect single-target echoes at close range.

When all echoes from all ranges are resolved, as often happens when transducers are lowered close enough to scattering layers, it is easy to compensate for the oversampling effect. It can be done by weighting each term in the Echo Value Constant estimators, or the mean backscattering cross-section estimator, by weights that are proportional to the inverse of the corresponding squared ranges. The estimators of the mean Echo Value Constant modified to compensate for the depth-oversampling effect is given in the Appendix. These estimators were not used here because cod were mainly distributed within a narrow depth range. When the echoes from the upper layers of a registration are completely resolved but start to overlap with each other deeper down, it is best to stratify the echoes with respect to depth and to estimate the mean Echo Value Constant and carry out echo-integration separately for each depth stratum, where this is possible.

I hope that the alternative echo-integration method presented here can give better, more-robust abundance estimates in many situations than other *in situ* methods, because it is based on the Echo Value Constant defined by integrated echo intensities instead of a backscattering cross-section defined from an echo's peak value. The concepts of the alternative method are expressed in terms of the space where the transducer is moved, and are simpler than

that of the classical method by being independent of the many traditional concepts applied in classical theory. With the introduction of the split-beam system and major improvements in signal-to-noise ratio and the dynamic range of echosounders, I believe that systems for acoustic observation have evolved beyond the theoretical methods for abundance estimation. The standard echo-integration method with its estimation of mean backscattering cross-section from catch samples does not use detection angles of single-target echoes systematically, except during calibration with spheres.

One example of a simple idea that has not yet been developed is that of counting fish within a known area by counting the number of echo traces within some fixed distance from the acoustic axis, although this method is likely to work well in many situations with low fish density or close-range detections. My prediction about acoustic-abundance estimation is that standard methods will in future be based on the use of transducers free to be moved in three dimensions. This situation will develop when acceptable power systems for free-swimming, remotely operated underwater vehicles are available. *In situ* and echo-counting methods may then be a natural choice for abundance estimation. Being able to select a favourable distance between the transducer and the scattering layers may be the only way to remove most of the sources of bias inherent in *in situ* methods.

In conclusion, the fact that the alternative and classical methods of acoustic-abundance estimation give almost equal mean estimates of cod density is a strong indication that one method is not biased relative to the other. It also suggests that the mathematical derivation of estimators (7) and (9) of Aksland (2005), with specifications and modifications as used here, are correct. However, estimator (8), i.e. estimator (9) of Aksland (2005), is not recommended for use without modification, because the assumptions behind it as an estimator are not likely to be fulfilled by the echo data.

Acknowledgements

I thank Egil Ona at the Institute of Marine Research (IMR), Bergen, Norway, for providing the file of raw data used in this paper, and for making the computations by the classical echo-integration method that allowed the comparisons herein to be made. An anonymous referee is also thanked for providing many useful comments on an early draft of the manuscript.

References

Aksland, M. 1976. Estimators in acoustic surveying of fish populations. ICES CM 1976/B: 36.

Aksland, M. 1983. Acoustic-abundance estimation of the spawning component of the local herring stock in Lindaas-pollene, western Norway. Fiskeridirektoratets Skrifter Serie Havundersøkelser, 17: 297–334.

Aksland, M. 1986. Estimating numbers of pelagic fish by echo integration. Journal du Conseil Conseil International pour l'Exploration de la Mer, 43: 7–25.

Aksland, M. 2005. An alternative echo-integrating method. ICES Journal of Marine Science, 62: 226–235.

Clay, C. S. 1983. Deconvolution of the fish scattering PDF from the echo PDF for a single-transducer sonar. Journal of the Acoustical Society of America, 73: 1989–1994.

Demer, D. A., Soule, M. A., and Hewitt, R. P. 1999. A multiple-frequency method for potentially improving the accuracy and precision of *in situ* target-strength measurements. Journal of the Acoustical Society of America, 105: 2359–2376.

Gauthier, S., and Rose, G. A. 2001. Diagnostic tools for unbiased *in situ* target-strength estimation. Canadian Journal of Fisheries and Aquatic Sciences, 58: 2149–2155.

Jech, J. M., Foote, K. G., Chu, D., and Hufnagle, L. C. 2005. Comparing two 38-kHz scientific echosounders. ICES Journal of Marine Science, 62: 1168–1179.

Korneliussen, R. 2004. The Bergen echo-integrator, post-processing system, with focus on recent improvements. Fisheries Research, 68: 159–169.

Korneliussen, R. J., and Ona, E. 2003. Synthetic echograms generated from the relative echo frequency response. ICES Journal of Marine Science, 60: 636–640.

Logerwell, E. A., and Wilson, C. D. 2004. Species discrimination of fish using frequency-dependent acoustic backscatter. ICES Journal of Marine Science, 61: 1004–1013.

Ona, E., and Barange, M. 1999. Single-target recognition. *In* Methodology for Target-Strength Measurements (with Special Reference to *In Situ* Techniques for Fish and Mikro-nekton) (ch. 5), Ed. by E. Ona. ICES Cooperative Research Report. 235 pp.

Reynisson, P. 1999. Split-beam method. *In* Methodology for Target-Strength Measurements (with Special Reference to *In Situ* Techniques for Fish and Mikro-nekton) (ch. 6), Ed. by E. Ona. ICES Cooperative Research Report. 235 pp.

Soule, M. A., Barange, M., and Hampton, I. 1995. Evidence of bias in estimates of target strength obtained with a split-beam echosounder. ICES Journal of Marine Science, 52: 139–144.

Urick, R. J. 1983. Principles of Underwater Sound, 3rd edn. McGraw-Hill, New York. 423 pp.

Appendix

Modified estimators for mean Echo Value Constant that compensate for depth-oversampling

When observing scattering layers acoustically at close range it may be possible to obtain an echo signal consisting of practically no overlapping single-target echoes. Because of the geometric spread of the beam, however, the number of echoes from different depths within the layer tends to be proportional to the square of the depth, as measured by the transducer. A sample of single-target echoes from the scattering layer will, therefore, be skewed relative to depth, and cause biased estimates if backscattering power or target-strength distribution changes with depth. This source of bias may be serious if the ratio between the bottom and top depths of the layer is large. This is the reason for giving modified estimators of the mean Echo Value Constant that compensate for depth-oversampling.

Let z and r denote depth and range to a target measured from the transducer, respectively. Then, $z = r \cos \theta$, where

θ is the observation aspect of the target. Estimators (8) and (9) of Aksland (2005) are

$$\widehat{\Psi}_3 = \frac{\pi \tan^2 \theta_0}{n-m} \sum_1^n w_i \cos^2 \theta_i,$$

and

$$\widehat{\Psi}'_3 = \frac{\pi \tan^2 \theta_c}{n} \sum_1^n w_i \cos^2 \theta_i.$$

Both can be written as

$$C \sum_1^n \frac{1}{n} w_i \cos^2 \theta_i,$$

where $1/n$ is the equal weight for each term, and constant C is different for the two estimators. The sum of these weights is 1.

To reduce the influence of the deep echoes, I replace the equal weights with depth-dependent weights proportional to the inverse of the expected number of echoes at depth, and which also sum up to 1. The weights

$$\frac{z_i^{-2}}{\sum_j z_j^{-2}}, \quad i = 1, 2, \ldots, n,$$

where z_i is the depth of the target for the ith echo, satisfy this. However, it is range r_i, where $z_i = r_i \cos \theta_i$, that is directly observed for each echo. Using this, the following alternative form for the estimators is obtained:

$$C \left[\sum_i r_i^{-2} \cos^{-2} \theta_i \right]^{-1} \sum_i r_i^{-2} w_i.$$

Note that the term $r_i^{-2} w_i$ is equal to the integrated echo intensity, with 20 log R TVG. The two alternative estimators are, therefore, given as

$$\widehat{\Psi}_4 = \pi \tan^2 \theta_0 \frac{n}{n-m} \left[\sum_i r_i^{-2} \cos^{-2} \theta_i \right]^{-1} \sum_i r_i^{-2} w_i, \quad \text{(A1)}$$

and

$$\widehat{\Psi}'_4 = \pi \tan^2 \theta_c \left[\sum_i r_i^{-2} \cos^{-2} \theta_i \right]^{-1} \sum_i r_i^{-2} w_i. \quad \text{(A2)}$$

Here estimator (A1) corresponds to estimator (8) of Aksland (2005), and estimator (A2) corresponds to estimator (9) of the same reference.

Now, estimator (7) will be modified. To compensate for the increasing number of echoes with depth, each term in expression (6) has to be divided by the square of the depth. Hence,

$$Q'(a) = \sum_{i=1}^n \theta_i^2 \left[\frac{w_i - a B_s^4(k\theta_i)}{z_i^2} \right]^2.$$

Also, using $z_i = r_i \cos \theta_i$, this gives

$$\widehat{a}' = \frac{\sum_i \theta_i^2 r_i^{-4} \cos^{-4} \theta_i w_i B_s^4(k\theta_i)}{\sum_i \theta_i^2 r_i^{-4} \cos^{-4} \theta_i B_s^8(k\theta_i)}. \quad \text{(A3)}$$

These estimators will not compensate adequately for depth-oversampling if the acoustic signals in part contain overlapping echoes, because the model used for the number of observed echoes with depth would then not hold.

Depth-oversampling of single-target echoes may also bias a mean scattering cross-section estimate based on *in situ* target-strength measurement. A similar compensation for this case using a weighted mean is straightforward.